

RESEARCH ARTICLE

Presynaptic A β 40 prevents synapse addition in the adult *Drosophila* neuromuscular junction

Begoña López-Arias, Enrique Turiégano, Ignacio Monedero, Inmaculada Canal, Laura Torroja*

Department of Biology, Universidad Autónoma de Madrid, Madrid, Spain

* laura.torroja@uam.es



OPEN ACCESS

Citation: López-Arias B, Turiégano E, Monedero I, Canal I, Torroja L (2017) Presynaptic A β 40 prevents synapse addition in the adult *Drosophila* neuromuscular junction. PLoS ONE 12(5): e0177541. <https://doi.org/10.1371/journal.pone.0177541>

Editor: William D Phillips, University of Sydney, AUSTRALIA

Received: September 22, 2015

Accepted: April 28, 2017

Published: May 16, 2017

Copyright: © 2017 López-Arias et al. This is an open access article distributed under the terms of the [Creative Commons Attribution License](https://creativecommons.org/licenses/by/4.0/), which permits unrestricted use, distribution, and reproduction in any medium, provided the original author and source are credited.

Data Availability Statement: Data are available from Figshare (https://figshare.com/articles/Raw_data_experiments_Lopez-Arias_et_al_2017_xlsx/1549716).

Funding: Support was provided by Fundación Centro de Investigación de Enfermedades Neurológicas - Fundación Reina Sofía Grant PI0006-08 to LT and IC; Ministerio de Ciencia y Tecnología (ES) grant BFU2008-04683-C02-02 to LT; Ministerio de Economía y Competitividad (ES) grant BFU2016-78327-P to LT. The funders had no

Abstract

Complexity in the processing of the Amyloid Precursor Protein, which generates a mixture of β amyloid peptides, lies beneath the difficulty in understanding the etiology of Alzheimer's disease. Moreover, whether A β peptides have any physiological role in neurons is an unresolved question. By expressing single, defined A β peptides in *Drosophila*, specific effects can be discriminated *in vivo*. Here, we show that in the adult neuromuscular junction (NMJ), presynaptic expression of A β 40 hinders the synaptic addition that normally occurs in adults, yielding NMJs with an invariable number of active zones at all ages tested. A similar trend is observed for A β 42 at young ages, but net synaptic loss occurs at older ages in NMJs expressing this amyloid species. In contrast, A β 42arc produces net synaptic loss at all ages tested, although age-dependent synaptic variations are maintained. Inhibition of the PI3K synaptogenic pathway may mediate some of these effects, because western analyses show that A β peptides block activation of this pathway, and A β species-specific synaptotoxic effects persists in NMJs overgrown by over-expression of PI3K. Finally, individual A β effects are also observed when toxicity is examined by quantifying neurodegeneration and survival. Our results suggest a physiological effect of A β 40 in synaptic plasticity, and imply different toxic mechanisms for each peptide species.

Introduction

Mounting evidences suggest that Alzheimer's disease (AD) is primarily a disease of synaptic dysfunction [1], and place the amyloid A β peptide as the culprit of AD etiology. Indeed, *in vivo* and *in vitro* studies have shown that A β interferes with synaptic plasticity: it impairs excitatory transmission, inhibits LTP and enhances LTD [2,3]; it leads to spine retraction and synaptic loss [2,4,5]; and it causes robust behavioral deficits, particularly in learning and memory [2,6,7]. However, there are still important opened questions as to exactly which A β peptide forms trigger these synaptic alterations.

The latest prevalent version of the amyloid hypothesis states that AD arises from synaptic toxicity mediated by amyloid peptide (A β) soluble oligomers [8,9]. Proteolytic processing of

role in study design, data collection and analysis, decision to publish, or preparation of the manuscript.

Competing interests: The authors have declared that no competing interests exist.

the APP transmembrane protein by β and γ secretases generates a mixture of A β species that differ by few amino acids in their C-terminal sequence. Currently, it is unclear whether synaptotoxicity in AD is attributable to single specific A β species or rather to a quantitatively and/or qualitatively defined combination [10], or even if individual species harbor different toxic activities. *In vitro* experiments using biochemically defined A β species provide insights into these questions, but their relevance to the *in vivo* situation remains unresolved. Moreover, recent data suggest that A β may have a physiological role in synaptic plasticity: synaptic activity increases A β production [11], A β is necessary for memory formation [12], and low concentrations of A β enhance LTP and memory formation [12–15]. However, whether this is actually the case and its implication to AD is still undetermined [16].

Drosophila has proven a useful model to address these questions, because toxicity of specific amyloid species can be dissected *in vivo* [17,18]. Expression of amyloid peptides in *Drosophila* neurons recapitulates many of the pathological hallmarks of AD, including progressive neurodegeneration and behavioral deficits. In general, the severity of the behavioral phenotype correlated with peptide aggregation propensity and *in vivo* toxicity measured by longevity, neurodegeneration, and mobility assays [19,20–24]. However, A β 40, which was proven non-toxic in these assays, induced early learning deficits in young flies [20,22].

The behavioral data suggest that all forms of A β , including A β 40, produce synaptic defects early in life, yet electrophysiological and structural studies *Drosophila* have reported synaptic alterations only in response to A β 42 or A β 42arc [19,20,25,26]. However, the effects of A β 40 on synaptic structure were assessed primarily in larval or pupal preparations. Because A β 40 affects olfactory learning, but have no obvious effects on other behavioral processes such as climbing ability, it may exert subtle alterations in adult synaptic plasticity. Moreover, the progressive nature of AD cognitive decline indicates that A β synaptotoxicity is age-dependent. Therefore, we aimed at finding a model that could uncover small changes in age-related synaptic dynamics elicited by particular A β species.

The *Drosophila* adult NMJ should provide a simple, reproducible and quantifiable system to examine alterations on synaptic dynamics. A few studies in the adult NMJ have described age-dependent morphological changes [27,28]. These changes are consistent with an early period of synaptic refinement and maturation, analogous to that described in the fly antennal lobes [29] and mushroom bodies [30], and with a subsequent phase of age-related motor decline [31,32]. Thus, we hypothesized that the adult ventral NMJ would provide a model suitable for studying how particular A β peptides affect age-dependent synaptic remodeling.

In this study, we systematically compared the age-dependent synaptotoxic effect of presynaptic secretable forms of A β 40, A β 42, or A β 42arc (a mutant form with increased aggregation propensity which causes early onset familial AD; [33]) in the *Drosophila* adult glutamatergic NMJ. We show that in wild type NMJs, there is an age-dependent variation in the number of active zones, which peaks at 15 days after eclosion. Our data shows that A β 40 blocks these changes, so that it renders a slightly reduced, but constant number of synapses throughout adult life. On the contrary, both A β 42 peptides cause net synaptic loss, albeit age-dependent variations are observed. These qualitative differences were apparent even in the presence of PI3K overexpression, which causes a dramatic increase in the number of synaptic contacts [34]. Our data provide new evidences of qualitative differences between the three A β peptides in their synaptotoxic activities, and suggest a physiological role for A β 40 in synaptic plasticity.

Materials and methods

Fly culture

Fly stocks used were: w^{1118} , $w^{1118};D42-GAL4$ -drives expression in all motor neurons and in some neuronal populations in the adult brain [35]-, and $w^{1118};elav-GAL4$ -drives panneural expression- (all from Bloomington *Drosophila* Stock Center <http://flystocks.bio.indiana.edu/>); $w^{1118};UAS-A\beta_{42}$, $w^{1118};UAS-A\beta_{42}Arc2E$, and $w^{1118};UAS-A\beta_{40}$ (generously donated by Dr. Crowther D.C., [21]); $w^{1118};UAS-PI3K^{92E}$ [36]. Lines harboring two *UAS* transgenes (A β and PI3K) were generated by standard genetic procedures.

For all experiments, males were analyzed from the progeny of crosses between *UAS* transgenic males and either $w^{1118};Gal4$ (experimental flies) or w^{1118} (control flies) females. The Gal4 control males were collected from a cross between $w^{1118};Gal4$ and w^{1118} . All crosses were kept at 26°C and parents transferred to new tubes every 2–3 days to maintain similar crowding conditions. When adults started to eclose, tubes were emptied and males collected after 24h and kept in tubes at 26°C for aging.

Longevity assay

Males of the specified genotypes were incubated at 26°C in groups of 20 in plastic vials and transferred every 2 days to fresh food. Death or lost flies were counted every 2 days. A minimum of five experiments per genotype was performed.

Dissection and immunohistochemistry

For neuromuscular junction (NMJ) analysis, ventral abdominal body-wall muscle preparations were dissected in Ca²⁺ free saline from 3, 7, 15, 20 and 30-day old adult males [37]. For assessing A β synaptotoxicity, we selected the ventral abdominal NMJ in the third abdominal hemisegment (Fig 1A). Samples were fixed in 4% formaldehyde in PBS, and immunostained with monoclonal antibody nc82 (anti-Bruchpilot 1:20, Developmental Studies Hybridoma Bank) visualized with α -mouse Alexa-488 (1:500, Invitrogen) and with Cy3-conjugated anti-HRP (1:200, Jackson Immuno Research). Anti-HRP signal reveals neuronal membranes, delimitating the motor neuron terminals. Bruchpilot is a CAST (CD3E-associated protein) homolog localized to the presynaptic specialization [38], and thus that was used to reveal active zones in the motor neuron terminal. Each A β -expressing genotype was processed simultaneously with its respective age-matched controls, to control for quantitative differences due to culture conditions.

Clearing of brain tissue for neurodegeneration assays

15 and 20 day old adults were decapitated and fly brains dissected in PBS and fixed for 30 minutes in 10% formalin in phosphate buffer (Electron Microscopy Sciences). After 3 washes in PBS (5 minutes each), samples were permeabilized in cold methanol (Panreac) for 5 minutes, treated with clearing solution (1:2 Benzyl Alcohol:Benzyol Benzoate, Sigma Aldrich) for another 5 minutes as described [39], and mounted in the same solution in excavated slides.

Image acquisition and quantification

Preparations were visualized using an Olympus IX70 confocal microscope. For body wall preparations, 1 μ m optical sections were taken. Stacks from hemisegments were used to quantify the number of Bruchpilot-containing active zones, with a macro-function developed in ImageJ that automatically selects the HRP-labeled motor terminal in each section and counts individual Bruchpilot-positive punctae while avoiding repeatedly counting the same synapse

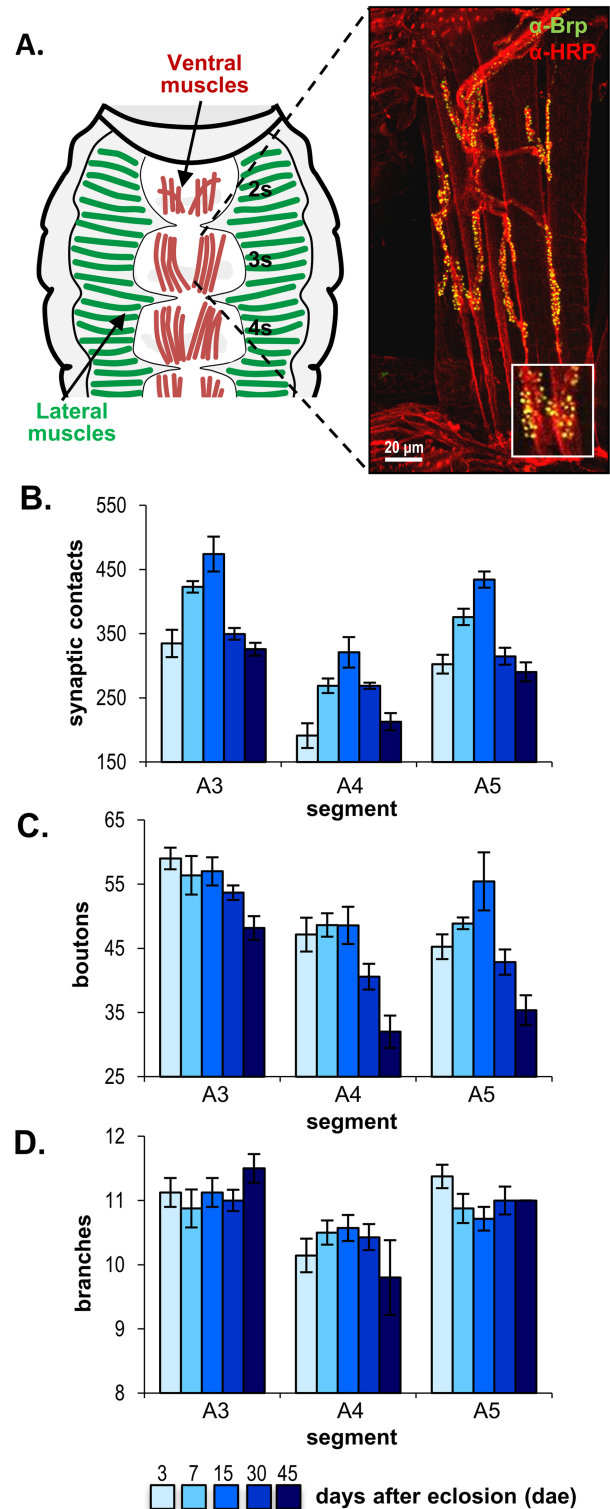


Fig 1. Age-dependent changes in the synaptic structure of the adult neuromuscular junction. (A) Schematic drawing of the anterior ventral abdomen (segments s2-s4), illustrating the position of the ventral abdominal muscles used for NMJ preparations. The accompanying image displays a representative confocal projection of a preparation labeled with anti-HRP (red) and anti-Brp (green). The inset shows active zones (synaptic contacts) at a higher magnification. Scale bar = 20 μ m. **(B-D)** Quantification of the number of active zones (synaptic contacts) **(B)**, boutons **(C)**, and branches **(D)** in control males in three different abdominal

segments (A3, A4, and A5) at five ages (3, 7, 15, 30, and 45 days after eclosion (dae)). Statistical analyses showed that the three parameters showed segmental differences, but only synapses and boutons displayed age-dependent variations, that were similar in all segments. Number of synaptic contacts differed between the three segments, for boutons only segment A3 was statistically different from the other two segments, while branches was different in A4. Number of NMJs analyzed was between 7 and 9 for each segment/age pair, except for 45 days, which was 6 for A3, 5 for A4, and 3 for A5. Each data point represents the average \pm SEM.

<https://doi.org/10.1371/journal.pone.0177541.g001>

in contiguous sections. Number of boutons (ellipsoid enlargements of the HRP-labeled axon terminal) and branches (defined as number of HRP-labeled axonal branch tips per hemisegment) was manually quantified based on the anti-HRP signal using the ImageJ point picker tool.

Autofluorescence from whole brains was recorded with an argon 488 nm laser in 2 μ m optical sections. To quantify brain neurodegeneration, a macro function was developed in Fiji-win32 to automatically detect black circular areas (holes of neurodegenerated tissue) in each autofluorescent section of the brain and measure the area of neurodegeneration relative to the total brain area.

Western blot

To measure total A β content, 10 heads of 15-day-old males of each genotype were homogenized in 20 μ l of lysis/monomerization buffer (9M Urea, 1% SDS, 1mM EDTA, 25 mM Tris-HCL pH 7.5), sonicated with 3–4 pulses of 5 seconds, heated at 55°C during 1 hour, and centrifuged for 2 minutes. The supernatant was collected and proteins were separated by SDS-PAGE in 10–20% Tris-Tricine precast gels (Bio-Rad) and electroblotted onto 0.22 μ m nitrocellulose membranes. The membrane was boiled in 1xPBS for 1 minute, and incubated with monoclonal anti-A β 6E10 (1:2000; Covance) and anti- α Tubulin (1:2000, Sigma) and visualized by enhanced chemiluminescence (ECL, Amersham) in a Bio-Rad GelDoc XR+ system. Quantification was performed with ImageJ, and amount of A β signal relative to tubulin was averaged from three experiments.

Levels of phospho-Akt and phospho-GSK3 β were used as readouts of PI3K activation. For this, 10 heads of 15-day-old males of each genotype were homogenized in 20 μ l of RIPA buffer containing a cocktail of protease inhibitors and phosphatase inhibitors, and centrifuged for 2 minutes. The supernatant was collected and proteins were separated in Any kD TGX precast gels (Bio-Rad), and electroblotted onto 0.22 μ m nitrocellulose membranes. Membranes were incubated with rabbit anti phospho(S505)-Akt or rabbit anti phospho(S9)-GSK3 β (both 1:1000; Cell Signaling Technology) and visualized by enhanced chemiluminescence (ECL, Amersham) with a Bio-Rad Gel Doc documentation system. After stripping, the same membranes were used to measure rabbit anti *Drosophila* Akt or mouse anti GSK3 β signals (both 1:1000; Cell Signaling Technology). Stripped membranes were finally probed with mouse anti Tubulin α (1:2000; Sigma-Aldrich). Quantification was performed with ImageJ, and the ratio p-S505Akt/Akt or p-S9GSK3 β /GSK3 β was averaged from four experiments.

Data analysis

Parameters analyzed in NMJs were as follows: number of synaptic contacts, defined as Bruchpilot-positive active zones (also referred as synapses); number of boutons; number of branches; ratio synapses/bouton; and A β -induced synaptic reduction, which represents the percentage of active zones lost in each A β -expressing genotype with respect to the average number of synapses in age-matched controls ([“average #synaptic contacts in controls”–“#synaptic contacts in A β ”]/ “average #synaptic contacts in controls”). For genotypes expressing only A β peptides,

A β -induced synaptic reduction was calculated relative to UAS controls, which showed a slightly lower synaptic count than Gal4 controls, and thus provided a conservative measure. For flies expressing A β and PI3K, synaptic reduction was calculated with respect to age-matched PI3K-expressing NMJs. To control for possible GAL4 titration effects that could reduce the levels of PI3K when expressed in conjunction with A β , nlsGFP instead of A β was co-expressed with PI3K (*w;UAS-PI3K/+; D42-Gal4 UAS-GFPnls/+*), and the number of synaptic contacts in 15 day-old flies was compared to age-matched *w;UAS-PI3K/+;D42-Gal4/+* flies. Statistical analysis showed no significant difference between both genotypes (number of synaptic contacts: 1035.7 ± 47.3 for *w;UAS-PI3K/+; D42-Gal4/+* $n = 10$ NMJs (9 flies); 988.7 ± 44.6 for *w;UAS-PI3K/+;D42-Gal4 UAS-GFPnls/+* $n = 12$ NMJs (7 flies); $t_{20} = 0.72$, $p = 0.48$).

For NMJ parameters and neurodegeneration, we tested for the normality of all variables and their usual logarithmic transformation. Statistical significance was calculated for the normally distributed variables with a two-way ANOVA test followed by Bonferroni *post hoc*. Data that did not meet the normality assumption were analyzed with Kruskal-Wallis non-parametric test. Because there is not a widely accepted non-parametric test to analyze the effect of interaction between factors, we also performed ANOVAs on these data, considering that the results obtained with ANOVA and Kruskal-Wallis test were equivalent. The SPSS 15.0.1 software (SPSS Inc., USA) was used throughout. Data are presented as average \pm SEM, and statistical functions are reported as $F_{g,N-1}$ for the ANOVA analysis and $H_{g,N}$ for the Kruskal-Wallis test, where N refers to the number of samples and g to the degrees of freedom. For regression analysis, we used the Real Statistics Resource Pack software (Release 3.5; Copyright (2013–2015) Charles Zaiontz; www.real-statistics.com) on Excel (Microsoft).

Differences in survival were analyzed using the Kaplan-Meier survival plots and log-rank analysis with the online survival analysis package OASIS [40]. Statistical significance was set at a corrected Bonferroni p value of 0.05.

Results

Age-dependent variations in the number of active zones in the adult *Drosophila* NMJ

Two studies in adult flies suggest that the fly NMJ undergoes morphological changes during the adult life [27,28]. While boutons enlarge throughout the adult life, branches elongate during the first two weeks but become shorter and thinner from this relatively young age onward [27]. The number of active zones was shown to increase during the first 5 days after eclosion [28], although this synaptic trait has not been analyzed at older ages. To characterize age-dependent synaptic structural changes in the *Drosophila* adult abdominal ventral NMJ (Fig 1A; [37]), we measured the number of branches, boutons, and Bruchpilot-positive active zones (referred to as number of synaptic contacts) in segments A3 to A5 at different ages between 5 and 45 days after eclosion (Fig 1), and analyzed the effect of segment, age, and their interaction on these variables with ANOVA (synapses and boutons) or Kruskal-Wallis (branches) tests.

The three parameters showed segmental differences (synapses: $F_{2,91} = 82.735$, $p < 0.001$; boutons: $F_{2,91} = 34.086$, $p < 0.001$; branches: $H_{(2,N=106)} = 17.807$, $p < 0.001$; Fig 1). However, only synapse and bouton number showed significant age-dependent differences (synapses: $F_{4,91} = 36.178$, $p < 0.001$; boutons: $F_{4,91} = 14.833$, $p < 0.001$; branches: $H_{(4,N=106)} = 1.343$, $p = 0.854$). Synapses continuously increased from 3 to 15 days after eclosion (dae), decreased from 15 to 30 dae and stabilized until at least 45-days of age (Fig 1B). For boutons, the number remained essentially constant until 15 dae, and decreased by 45 dae (Fig 1C). A similar temporal pattern was observed in all segments, as revealed by the lack of effect of the interaction

segment*age in the statistical analyses (synapses: $F_{8,91} = 1.237$, $p = 0.287$; boutons: $F_{8,91} = 1.450$, $p = 0.187$; branches: $F_{8,91} = 1.641$, $p = 0.124$).

Our data shows that in the ventral abdominal NMJ, net synaptic addition occurs during the first two weeks after eclosion, while net synaptic elimination prevails afterwards in the aging fly. Thus, this adult NMJ arises as a simple suitable model for analyzing age-dependent alterations in synaptic dynamics due to A β expression. To differentiate physiological age-dependent changes from A β -induced synaptic alterations, the two temporal phases of synaptic remodeling will be referred to as “age-dependent synaptic addition” and “age-dependent synaptic elimination”.

Presynaptic A β 40 prevents synapse addition in the adult NMJ, while A β 42 and A β 42arc yield net synaptic elimination

To examine how A β influences synapses during ageing, we performed a systematic quantitative analysis comparing the effect of presynaptic A β 40, A β 42 and A β 42arc on the morphology of the adult NMJ at different ages between 3 and 30 dae. Measures were taken at segment A3 and the effects of peptide (genotype), age, and their interaction, were statistically analyzed (Figs 2 and 3, Table 1).

Our results provide the first demonstration for a synaptic structural defect induced by A β 40 on *Drosophila* synapses (Fig 2A; Table 1). All three peptides caused a significant synaptic reduction from 7 dae on. At 3 dae, A β 40 and A β 42arc also decreased synaptic contacts, while the number of active zones in A β 42-expressing NMJs was intermediate between controls and NMJs with A β 40, although it was not significantly different from either one. Consistent with its higher toxicity, A β 42arc showed the strongest synaptic reduction (Fig 2A and 2B; Table 1) at all ages tested (at 30 days after eclosion, most A β 42arc flies had died, and therefore this age was not analyzed). In contrast, A β 42 induced a larger synaptic reduction than A β 40 at 20 and 30 dae, but a similar effect at younger ages (Fig 2A and 2B). These peculiarities in A β -induced synaptotoxicity could not be solely attributed to quantitative differences in peptide levels, because western analysis showed similar levels of total A β 40 and A β 42arc at 15 dae (Fig 2F), yet a stronger synaptic reduction induced by the mutant peptide at this age. Overall, these data suggests that all amyloid species show an early tendency to decrease synapses, which is consistent with reported learning defects induced by the three A β peptides at young ages [22,23].

An intriguing observation was that the number of active zones in A β 40-expressing NMJs remained constant throughout the ages tested. Indeed, statistical analyses showed an effect of the interaction between peptide type (genotype) and age on synapses (Table 1), denoting that A β expression alters the age-dependent changes of synapse number that occurs in physiological conditions. To further explore this question, we approximated the rate of synaptic change by the slope of the linear regression for the dataset covering the phase of age-dependent synapse addition (from 3 to 15 dae), and of age-dependent synapse elimination (from 15 to 30 dae; 15–20 dae for A β 42arc)(Table 2).

In control NMJs, the age-dependent synaptic addition occurring from 3 to 15 dae rendered a slope with a positive value, while the age-dependent synaptic elimination that occurs between 15 and 30 dae yielded a negative slope (Table 2). The synaptic temporal pattern of A β 40-expressing NMJs produced a slope which was not different from 0 for both age segments, and which was statistically different from both control regression lines (Table 2). Moreover, *post hoc* analyses identified A β 40 as the only genotype in which the number of active zones did not differ between ages, while all other genotypes showed age dependent variations (Fig 2A). These data demonstrate that the effect of A β 40 is qualitatively different from the

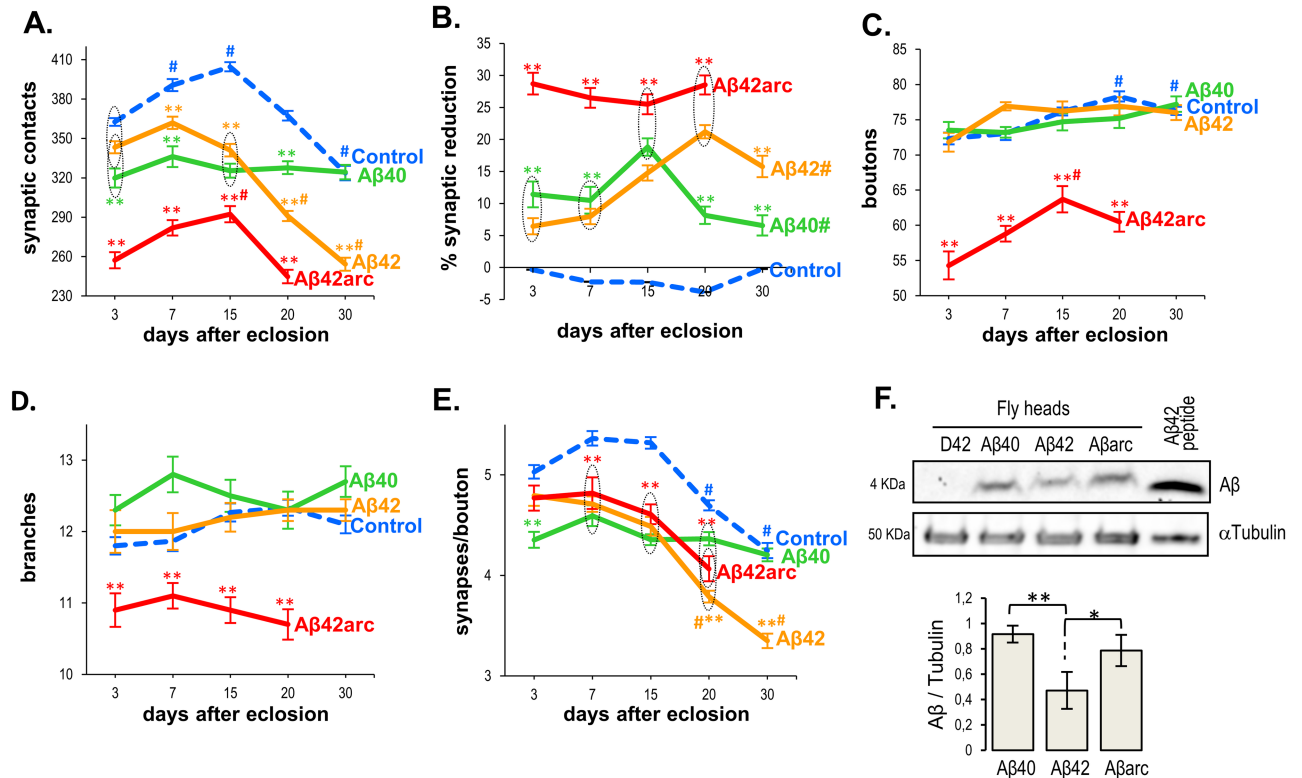


Fig 2. Age-dependent effects of three Aβ peptides on the synaptic structure of the adult neuromuscular junction. Parameters were quantified in the adult A3 ventral NMJ at 3, 7, 15, 20, and 30 days after eclosion (dae), in males expressing Aβ40, Aβ42, or Aβ42arc in motoneurons (*w; D42-Gal4/UAS-Aβ**) or in control males (*w; D42-Gal4/+ and w; UAS-Aβ*/+*). For simplicity, only the Gal4 control, common to all experimental genotypes, is shown. Parameters measured were (A) number of synaptic contacts, (B) percentage of synaptic reduction measured as: (average number of synaptic contacts in control – number of synaptic contacts in Aβ*)/average number of synaptic contacts in control, (C) number of boutons, (D) number of branches, and (E) ratio of synaptic contacts per bouton. Each data point represents the average of 10 hemisegments of the same genotype/age ±SEM. Asterisks denote significant differences (** p<0.001) with their respective age-matched controls (Gal4 and UAS) and the other Aβ-expressing genotypes. Circled discontinuous lines surround data points that are not statistically different between each other but are statistically different with the other data points outside the circle. The symbol # indicates that *post hoc* analyses detected statistical differences (p<0.01) within each particular genotype between data from that age and data from 3 dae. Notice that the number of synapses in Aβ40-expressing NMJs (A) remains constant throughout all ages tested, while it shows age-dependent variations for the other genotypes. Number of flies analyzed, N, is larger than 20 for all ages in the control genotype except for 30 dae (N = 16). For all Aβ*-expressing genotypes N = 8, except for: *w; D42-Gal4/UAS-Aβ40* 20 dae (N = 9); *w; D42-Gal4/UAS-Aβ42* at 7 and 30 dae (N = 9) and at 15 dae (N = 7); *w; D42-Gal4/UAS-Aβarc* at 7 and 15 dae (N = 9) and at 3 and 30 dae (N = 7). (F) Detection of total Aβ peptide (4 KDa) by western blot in head homogenates from 15 day-old flies expressing Aβ40, Aβ42, Aβ42arc (Aβarc), or from Gal4 control flies (D42). The right lane contains purified Aβ42 mixed with extract from control fly heads. αTubulin (50 KDa) was used to control for total protein content. Amount of Aβ was normalized with respect to αTubulin. Each data point in the graph represents the average from 3 experiments ±SEM. ** p<0.01, * p<0.05.

<https://doi.org/10.1371/journal.pone.0177541.g002>

other Aβ peptides. But more importantly, the results suggest that Aβ40 restrains the addition of new synapses that normally occurs during the first days of adult life.

For Aβ42-expressing NMJs, regression analysis revealed a modification in the temporal biphasic pattern of active sites. At young ages, from 3 to 15 dae, the rate of synaptic change was not different from 0 or from Aβ40, but differed from controls (Table 2). This suggests that in early adulthood, Aβ42 acts similarly to Aβ40, hindering synapse addition. In contrast, from 15 to 30 dae, age-dependent synaptic elimination occurred in Aβ42-expressing NMJs at a rate not different from controls (Table 2), suggesting a transformation in the synaptic action of this peptide with aging. Alternatively, the lower peptide content detected in Aβ42-expressing fly heads could account for its reduced early synaptotoxicity, while its age-dependent

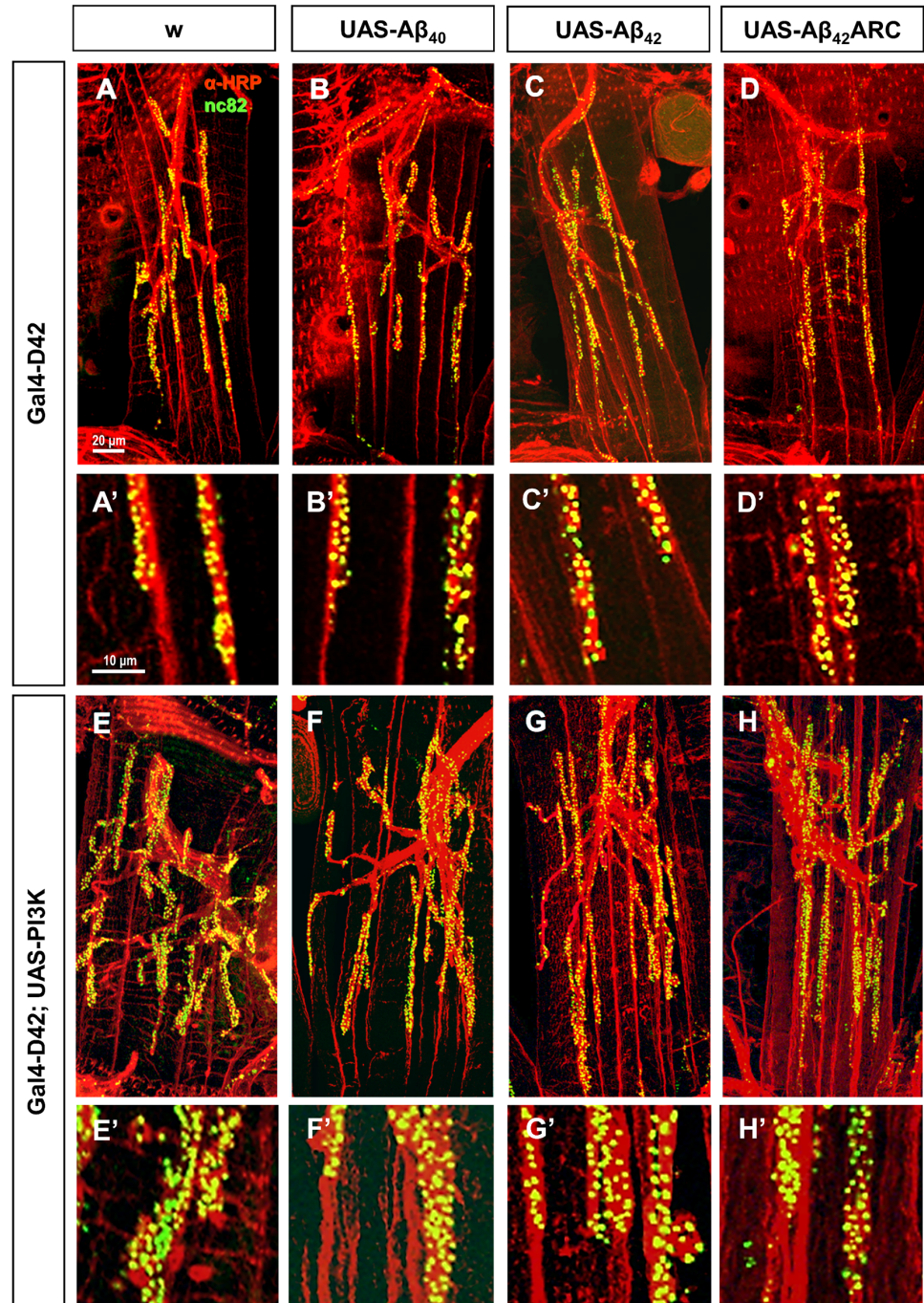


Fig 3. Morphology of 15-day-old fly NMJs expressing amyloid peptides, with or without elevated PI3K levels. Representative images showing active zones (green; anti-Bruchpilot) and neuronal membrane (red; anti-HRP) of A3 abdominal ventral NMJs from 15-day-old control males (w, A and E), and males expressing A β 40 (B and F), A β 42 (C and G), or A β 42arc (D and H), with normal (A-D) or elevated (E-H) levels of PI3K. Genotypes analyzed were (A) w; *D42-Gal4/+*, (B-D) w; *D42-Gal4/UAS-A β **, (E) w; *D42-Gal4/UAS-PI3K*, and (F-H) w; *D42-Gal4/UAS-PI3K, UAS-A β **. The complete NMJ is shown in images A-H (scale bar 20 μ m), and higher magnification of part of the NMJ is shown in images A'-H' (scale bar 10 μ m).

<https://doi.org/10.1371/journal.pone.0177541.g003>

Table 1. Summary of statistical results for the effect of different Aβ species on parameters of the adult neuromuscular junction.

	GENOTYPE		AGE		GENOTYPE * AGE	
	F _{6,387}	p<0.001	F _{4,387}	p<0.001	F _{22,387}	p<0.001
SYNAPTIC CONTACTS	H _(6,N = 420) = 193.776	p<0.001	H _(4,N = 420) = 102.776	p<0.001		
BOUTONS	F _{6,387} = 92.355	p<0.001	F _{4,387} = 19.012	p<0.001	F _{22,387} = 1.513	p = 0.066
	H _(6,N = 420) = 108.558	p<0.001	H _(4,N = 420) = 64.466	p<0.001		
SYNAPSES/BOUON	F _{6,387} = 51.033	p<0.001	F _{4,387} = 104.446	p<0.001	F _{22,387} = 4.849	p<0.001
BRANCHES	F _{6,387} = 26.225	p<0.001	F _{4,387} = 3.038	p = 0.017	F _{22,387} = 0.993	p = 0.472
	H _(6,N = 420) = 105.150	p<0.001	H _(4,N = 420) = 20.452	p<0.001		
SYNAPTIC REDUCTION	F _{6,387} = 244.835	p<0.001	F _{4,126} = 2.273	P = 0.061	F _{7,126} = 5.023	p<0.001
	H _(6,N = 420) = 254.330	p<0.001	H _(4,N = 420) = 0.818	P = 0.936		

Data on synaptic parameters measured in the adult ventral abdominal NMJs at segment A3, from seven genotypes (*w;D42-Gal4/+*, *w;UAS-Aβ^{*}/+*, and *w;D42-Gal4/UAS-Aβ^{*}*, being Aβ^{*} either Aβ40, Aβ42, or Aβ42arc) and 5 ages (3, 7, 15, 20, and 30 days after eclosion (dae)) were used for the analysis. Data with normal distribution were analyzed with a two-way ANOVA (F) that tested the effect of two variables (age and genotype) and their interaction (age*genotype). For data with non-normal distribution, the effect of either genotype or age was analyzed with the non-parametric one-way Kruskal-Wallis test (H). In these cases, to analyze the effect of age*genotype interaction, a two-way ANOVA was also performed that tested the effect of genotype, age, and their interaction. Therefore, for non-normally distributed data, both ANOVA (F) and Kruskal-Wallis (H) tests results are included. A minimum of 10 NMJs was measured for each genotype and age (for details on number of flies analyzed, see Fig 2). The two subscripted numbers after F functions indicate the degrees of freedom for the between-group and within-group variance. For H function, the first subscript indicates the degrees of freedom.

<https://doi.org/10.1371/journal.pone.0177541.t001>

accumulation [21,22,24] would strengthen its toxic effects at older ages. In contrast to Aβ40 and Aβ42, expression of Aβ42arc yielded NMJs with an age-dependent rate of synaptic change statistically not different from controls at both age intervals (Table 2). These data demonstrate remarkable specific differences in the influence of age on the synaptic effects of each amyloid species.

For boutons and branches, only the Aβ42arc peptide showed a consistent significant effect (Fig 2C and 2D; Table 1). The reduction in the number of boutons (and/or branches) induced by Aβ42arc could account for its synaptic reduction, in which case the ratio of synapses per bouton should not differ from control NMJs. However, this ratio exhibited statistical

Table 2. Linear regressions examining the rate of synaptic change in control and Aβ-expressing NMJs during two age intervals.

Age interval	Regression Analysis						Slope comparisons		
	Genotype	b (slope)	t	df	p	R ²	t	df	p
3–15 dae	Control	2.825	6.778	98	<0.001*	0.319			
	Aβ40	0.202	0.245	28	0.806	0.002	2.921	126	0.004#
	Aβ42	-0.521	-0.825	28	0.417	0.024	3.925	126	<0.001#
	Aβ42arc	2.693	3.716	28	<0.001*	0.330	0.151	126	0.880
15–30 dae	Control	-5.135	-13.806	98	<0.001*	0.660			
	Aβ40	-0.111	-0.233	28	0.817	0.002	7.450	126	<0.001#
	Aβ42	-5.49	-10.712	28	<0.001*	0.804	0.520	126	0.604
	Aβ42arc (15–20 dae)	-9.5	-5.972	18	<0.001*	0.665	1.345	96	0.182

Linear regression analyses were performed for each genotype with data of the number of active zones pooled from 3 to 15 or from 15 to 30 (15 to 20 for Aβ42arc) days after eclosion (dae). We additionally performed six analyses comparing the slopes of the regression lines for each Aβ-expressing genotype with the slope obtained for the corresponding control genotype (“slope comparisons”).

* indicates that the slope of the regression line is significantly different from 0.

indicates that significant differences were found between the slopes.

<https://doi.org/10.1371/journal.pone.0177541.t002>

differences between all A β -expressing genotypes, including A β 42arc, and age-matched controls at most ages tested (Fig 2E), suggesting a specific impact of the peptide on synaptic contacts, independent of its influence on bouton and branch number.

A β peptides induce synaptic reduction in adult NMJs enlarged by PI3K over expression

Presynaptic activation of the PI3K pathway promotes synaptogenesis both in *Drosophila* and mammals [34,41], while reducing the activity of the pathway, or increasing GSK3, a target inhibited by the pathway, has the opposite effect [34]. This pathway is altered in patients with Alzheimer's disease, which show increased GSK3 activity, a condition that is thought to directly contribute to AD synaptic dysfunction [42,43]. Thus, we wondered whether PI3K activation might counteract A β induced synaptotoxicity. To test this, we overexpressed the PI3K catalytic subunit, Dp110, in motor neurons together with single A β species, and analyzed their combined effect on the adult NMJ. Synaptic morphological parameters were measured at 15 and 20 dae, two ages at which each A β peptide shows clear differences with respect to controls and to the other amyloid species (Figs 3 and 4, Table 3).

Consistent with previous findings on the *Drosophila* larval NMJ and central adult synapses [34], overexpression of PI3K lead to a robust expansion of the adult NMJ, which showed increased number of synaptic contacts, boutons and branches at both ages relative to controls with normal PI3K levels (Figs 3 and 4). The ratio of synapses per bouton also increased (Fig 4D), supporting independent mechanisms to regulate bouton and active zone formation. Interestingly, the number of synaptic contacts decreased from 15 to 20 dae (Fig 4A), therefore following the pattern of age-dependent variations observed in controls.

Simultaneous expression of PI3K and any of the three A β peptides also produced an increase in the number of active zones, boutons and branches when compared to A β expressing NMJs with normal PI3K levels, demonstrating that overactivation of the PI3K pathway can induce synaptic overgrowth even in the presence of A β peptides (compare Figs 2 and 4; Table 3). However, our data demonstrate that A β peptides can still exert their synaptotoxic effects on synapses with elevated PI3K levels, because synaptic parameters were significantly reduced in NMJs co-expressing PI3K and any of the three amyloid peptides when compared to NMJs expressing PI3K in the absence of A β (Fig 4).

In general, specific A β effects on active zones in NMJs overexpressing PI3K followed a similar tendency to that observed with normal PI3K levels, providing further support for the specific effects uncovered in this study (compare Figs 2 and 4). For example, A β 42arc induced the largest synaptic reduction also in the presence of elevated PI3K (A β 42arc: 37.3 \pm 9.2% at 15 dae, 39.2 \pm 6.1% at 20 dae; A β 40: 31.8 \pm 5.0% at 15 dae, 19.0 \pm 4.6% at 20 dae; A β 42: 22.9 \pm 7.3% at 15 dae, 17.8 \pm 9.4% at 20 dae). However, some differences were detected when assessing how the level of PI3K activity modifies amyloid outcome. First, *post hoc* analyses showed that amyloid peptides induced significantly larger synaptic reduction in the presence of elevated PI3K levels ($p < 0.0001$ for all three comparisons $D42;UAS-A\beta^*$ vs. $D42;UAS-A\beta^*$, $UAS-PI3K$). Second, as with normal PI3K levels, A β 42arc exerted the strongest effect on branch and boutons in conditions of elevated PI3K (Fig 4B and 4C), but deleterious effects of A β 40 and A β 42 on these structures also became significant when PI3K signaling was augmented ($p < 0.0001$ for all three comparisons $D42;UAS-A\beta^*$ vs. $D42;UAS-A\beta^*$, $UAS-PI3K$).

Noticeably, A β 40 also altered the age-dependent synaptic pattern when PI3K was overexpressed, so that the number of active zones remained constant between 15 and 20 dae (Fig 4A). This confirms our initial observations with normal PI3K levels, and provides strong support for a specific role of A β 40 in opposing synapse addition during synaptic refinement.

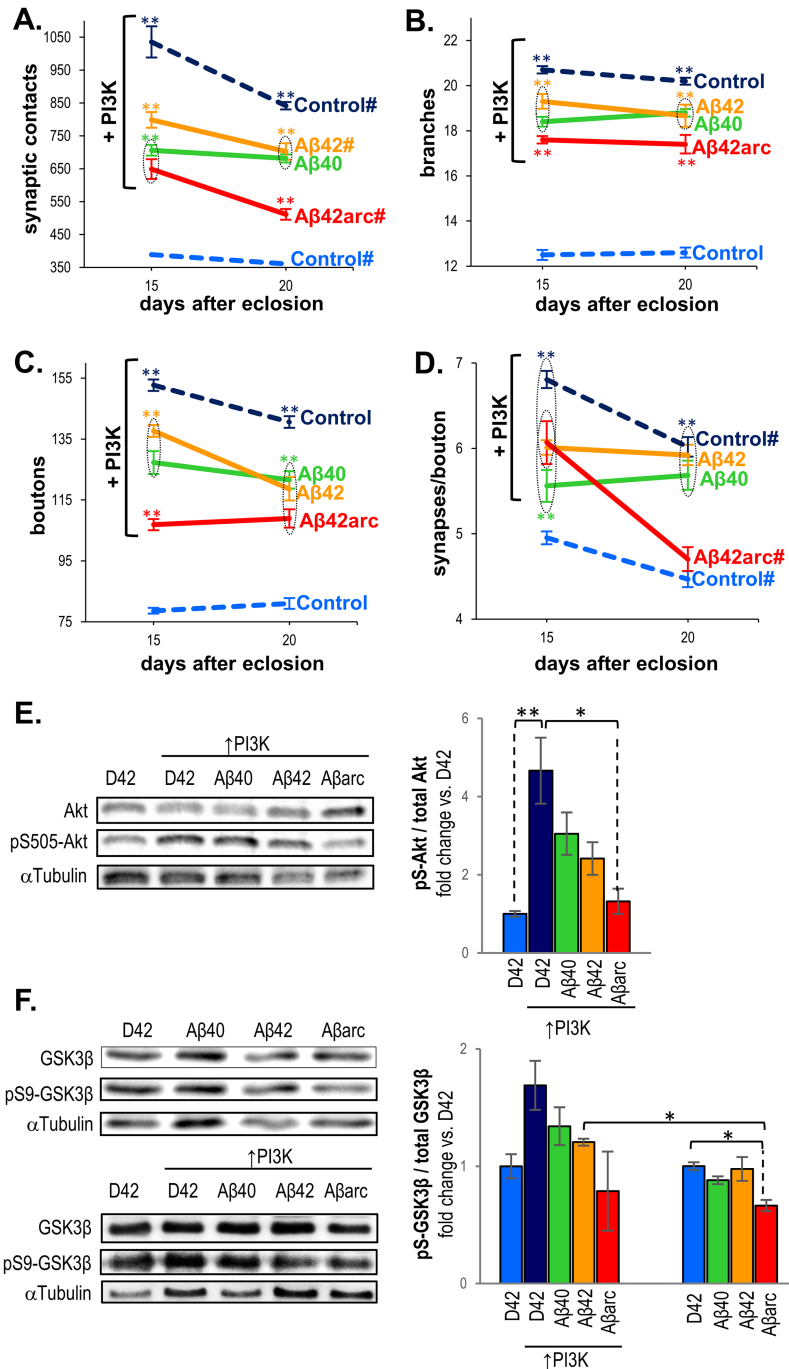


Fig 4. Specific effects of the three amyloid peptides on synaptic structure persists in expanded adult neuromuscular junctions over expressing PI3K. (A–D) Parameters were quantified in the adult A3 ventral NMJ at 15 and 20 days after eclosion, in males overexpressing in motor neurons: PI3K (*w; D42-Gal4/UAS-PI3K*), PI3K and either A β 40, A β 42, or A β 42arc (*w; D42-Gal4/UAS-PI3K UAS-A β **), and in control males (*w; D42-Gal4/+* and *w; UAS-PI3K UAS-A β */+*). For simplicity, only the Gal4 control, common to all experimental genotypes, is shown (light blue line). Parameters measured were (A) number of synaptic contacts, (B) number of branches, (C) number of boutons, and (D) ratio of synaptic contacts per bouton. Each data point represents the average of 8–10 hemisegments of the same genotype/age \pm SEM. Asterisks denote significant differences (** $p < 0.01$) with their respective age-matched controls (Gal4 and UAS), and the other A β -expressing. The symbol # associated to the genotype label indicates that *post hoc* analyses detected statistical differences ($p < 0.01$) between the two ages within that particular genotype. Notice that the number of synapses in A β 40-expressing NMJs (A) remains constant from 15 to 20 dae, while it shows age-dependent

variations for the other genotypes. Discontinuous circles surround data points that are not statistically different between each other but statistically different with the other data points outside the circle. The number of flies analyzed was N = 8, except for: *w; D42-Gal4/+* 15 dae (N = 9); *w; D42-Gal4 / UAS-PI3K* 15 dae (N = 9); *w; D42-Gal4 / UAS-PI3K UAS-Aβ40* 15 dae (N = 9); *w; D42-Gal4 / UAS-PI3K UAS-Aβ42* 20 dae (N = 7); *w; D42-Gal4 / UAS-PI3K UAS-Aβ42arc* 15dae (N = 9) and 20 dae (N = 7). (E) Representative blots showing detection of pS505-Akt and total Akt in head homogenates from 15 day-old flies expressing PI3K (*w; D42-Gal4/UAS-PI3K*), PI3K and either Aβ40, Aβ42, or Aβ42arc (*w; D42-Gal4 / UAS-PI3K UAS-Aβ**), and in control males (*D42, w; D42-Gal4/+*). Graph depicts fold changes of the ratio pS505-Akt/total Akt relative to control males. (F) Representative blots showing detection of pS9-GSK3β and total GSK3β in head homogenates from 15 day-old flies expressing each Aβ peptide (*w; D42-Gal4 / UAS-Aβ**), PI3K and either Aβ40, Aβ42, or Aβ42arc (*w; D42-Gal4 / UAS-PI3K UAS-Aβ**), PI3K in the absence of Aβ (*w;D42-Gal4/ UAS-PI3K*), and in control males (*D42, w; D42-Gal4/+*). Graphs depict fold changes of the ratio pS9-GSK3β/ GSK3β relative to control males. Anti Tubulin α was used for signal normalization in all blots. Each data point in the graphs represents the average from 4 experiments ±SEM. ** p<0.001, * p<0.01.

<https://doi.org/10.1371/journal.pone.0177541.g004>

Our data show that the synaptotoxic effects of each Aβ peptide persist in NMJs overexpressing PI3K. Aβ peptides have been reported to inhibit the PI3K pathway both *in vivo* and in cell culture [25,44,45]. Hence, the observed Aβ induced synaptic reduction in flies with elevated PI3K may be mediated by inhibition of the PI3K synaptogenic pathway. We therefore compared the activity of the PI3K pathway in 15 day-old flies co-expressing PI3K and each Aβ peptide. For this purpose, we quantified the degree of phosphorylation of Akt, the main effector kinase of the pathway, and the level of inhibitory phosphorylation of GSK3β, a target of the pathway especially relevant to AD. Over expression of PI3K alone induced a marked increase of the ratio p-S505Akt/Akt when compared with flies with normal PI3K levels (Fig 4E). All three peptides showed a tendency to reduce this ratio, albeit this reduction was statistically significant only for the Aβ42arc peptide (Fig 4E). A similar trend was observed for GSK3β inhibitory phosphorylation, but differences were not statistically significant for any of the genotypes (Fig 4F). These data suggest that in NMJs with elevated PI3K levels, amyloid peptides can

Table 3. Summary of statistical results for the effect of different Aβ species with normal or elevated PI3K levels, on parameters of the adult neuromuscular junction, at 15 and 20 days after eclosion.

	GENOTYPE		AGE		GENOTYPE*AGE	
	F _{14,326}	p	F _{1,326}	p	F _{14,326}	p
SYNAPTIC CONTACTS	F _{14,326} = 457.206	p<0.001	F _{1,326} = 138.497	p<0.001	F _{14,326} = 8.309	p<0.001
	H(14,N = 356) = 268.191	p<0.001	H(1,N = 356) = 33.947	p<0.001		
BOUTONS	F _{14,326} = 292.856	p<0.001	F _{1,326} = 7.031	p = 0.008	F _{14,326} = 4.609	p<0.001
	H(14,N = 356) = 140.761	p<0.001	H(1,N = 356) = 1.006	p = 0.316		
SYNAPSES/BOUTON	F _{14,326} = 47.843	p<0.001	F _{1,326} = 110.890	p<0.001	F _{14,326} = 4.603	p<0.001
	H(14,N = 356) = 178.545	p<0.001	H(1,N = 356) = 58.535	p<0.001		
BRANCHES	F _{14,326} = 411.999	p<0.001	F _{1,326} = 1.233	p = 0.268	F _{14,326} = 1.014	p = 0.439
	H(14,N = 356) = 146.587	p<0.001	H(1,N = 356) = 0.017	p = 0.897		
SYNAPTIC REDUCTION	F _{14,326} = 47.782	p<0.001	F _{1,326} = 6.649	p = 0.010	F _{14,326} = 9.270	p<0.0017

Data on synaptic parameters measured in the adult ventral abdominal NMJs at segment A3, from fifteen genotypes (*w;D42-Gal4/+*, *w;UAS-Aβ*/+*, *w; UAS-PI3K/+*, *w;UAS-Aβ* UAS-PI3K/+*, *w;D42-Gal4/UAS-PI3K*, *w;D42/UAS-Aβ**, and *w;D42-Gal4/UAS-Aβ* UAS-PI3K*, being Aβ* either Aβ40, Aβ42, or Aβ42arc) and 2 ages (15 and 20 days after eclosion (dae)) were used for the analysis. Data with normal distribution were analyzed with a two-way ANOVA (F) that tested the effect of two variables (age and genotype) and their interaction (genotype*age). For data with non-normal distribution, the effect of either genotype or age was analyzed with the non-parametric one-way Kruskal-Wallis test (H). In these cases, to analyze the effect of age*genotype interaction, a two-way ANOVA was also performed that tested the effect of genotype, age, and their interaction. Therefore, for non-normally distributed data, both ANOVA (F) and Kruskal-Wallis (H) tests results are included. 8–10 NMJs were measured for each genotype and age (for details on number of flies analyzed, see Figs 2 and 4). The two subscripted numbers after F functions indicate the degrees of freedom for the between-group and within-group variance. For H function, the first subscript indicates the degrees of freedom.

<https://doi.org/10.1371/journal.pone.0177541.t003>

inhibit the PI3K pathway, opposing its synaptogenic activity. To test if a similar mechanism might explain the synaptotoxic effect of A β in NMJs with normal PI3K levels, we quantified inhibitory phosphorylation of GSK3 β in flies expressing each of the three A β species, and found a significant reduction only for NMJs expressing A β 42arc (Fig 4F). Together, our data suggest that in *Drosophila*, amyloid peptides can also block PI3K pathway activation, and that this inhibition contributes to synaptic loss.

PI3K over expression can partially rescue early neurodegeneration induced by A β 42, but not by A β 42Arc

Our previous results show that A β 40 and A β 42-derived peptides display qualitatively different synaptotoxic effects, which may be partially mediated by inhibition of the PI3K pathway. Data gathered from various studies in *Drosophila* suggest that A β -induced synaptic deficit, cell loss, locomotor decline, and reduced life span may be elicited by different mechanisms [19,22,23,46,47], which could have different requirements for PI3K signaling. To gain insights into this question, we analyzed how PI3K over expression influences A β effects on neurodegeneration and life span.

Neuroprotective roles have been well established for PI3K [48]. Because possible neuroprotective effects would be easier to detect at early phases of the neurodegenerative process, we quantified neurodegeneration at relatively early ages (15 and 20 dae), using a pan-neural driver and an automated image analysis tool that measured brain tissue loss in whole brains. Indeed, this technique allowed detection of significant neurodegeneration as early as 15 dae with A β 42-derived peptides (Fig 5), while prior experiments using very similar experimental conditions revealed first signs of neurodegeneration at 30 dae [22]. At these young ages, and despite the difference in peptide content (Fig 2F), the extension of the neurodegenerated area was similar in A β 42- and A β 42arc-expressing brains. Even though the two-way ANOVA detected significant age dependent differences, *post hoc* analyses did not reveal differences between 15 and 20 dae within each genotype. Flies expressing A β 40 or PI3K, or both, were not significantly different from controls (Fig 5I), and thus did not evidence brain tissue loss.

Importantly, overexpression of PI3K was able to reduce A β 42-induced neurodegeneration to almost wild type levels at both ages (Fig 5I). On the contrary, toxicity of A β 42arc was not influenced by PI3K levels at any of the two ages tested (Fig 5I). These results are consistent with the level of PI3K pathway activity measured by Akt phosphorylation (Fig 4E), which show higher activity levels in A β 42 than in A β 42arc expressing flies, and suggest that activation of this pathway can protect against A β -induced cytotoxicity.

We next tested if PI3K positively affected life span in males expressing each of the A β peptides. Although most controls showed undistinguishable cumulative survival curves (Fig 6), there were significant differences in some control lines which complicated interpretation of the results. *UAS-PI3K* control flies displayed an abnormally high survival ($p < 0.001$ vs. all other genotypes), while *D42-Gal4* control males had slightly reduced survival when compared to the other control genotypes ($p < 0.001$ vs. all other control genotypes). Life span of flies overexpressing PI3K alone was undistinguishable from the Gal4 control ($\chi^2 = 1.03$, $p = 1$), but lower than the other control genotypes ($p < 0.001$).

Consistent with previous reports [21,22,26,46], expression of A β 40 did not reduce life span, not even in the presence of overexpressed PI3K (Experiment A β 40 vs. Experiment A β 40 +PI3K: $\chi^2 = 0.22$, $p = 1$) (Fig 6A). Furthermore, longevity of A β 40 flies, with or without elevated PI3K levels, was higher than Gal4 controls (Control Gal4 vs. Experiment A β 40: $\chi^2 = 11.36$, $p = 0.011$; Control Gal4 vs. Experiment A β 40+PI3K: $\chi^2 = 10.38$, $p = 0.018$) and flies expressing PI3K alone (Experiment PI3K vs. Experiment A β 40: $\chi^2 = 16.65$, $p < 0.001$; Experiment PI3K vs.

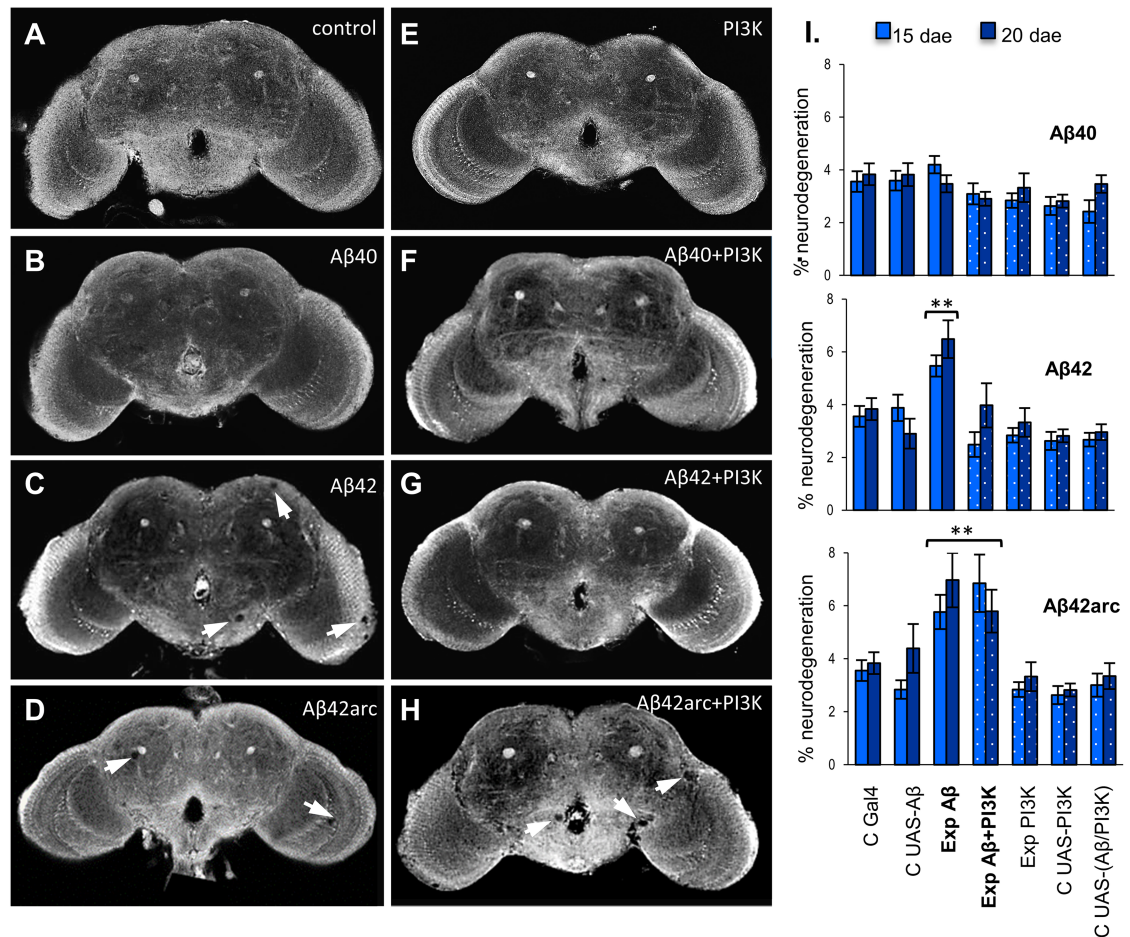


Fig 5. Effect of neuronal expression of three amyloid peptides, with or without elevated PI3K levels, on adult neurodegeneration. (A-H) Representative sections of cleared whole brains from 20-day old control males (A and E), and males expressing Aβ40 (B and F), Aβ42 (C and G), or Aβ42arc (D and H), with normal (A-D) or elevated (E-H) levels of PI3K. Arrows point to holes of neurodegenerated tissue. (I) The percentage of neurodegenerated area was measured at 15 and 20 days after eclosion (dae) in whole brains from males expressing Aβ40, Aβ42, or Aβ42arc with normal (Exp Aβ) or elevated levels of PI3K (Exp Aβ+PI3K), and control (C *) and PI3K-overexpressing (Exp PI3K) males. Control genotypes were as follows: C Gal4—*w;elav-Gal4/+*, C UAS-Aβ - *w;UAS-Aβ*/+*, C UAS-PI3K - *w;UAS-PI3K/+*, C UAS-(Aβ/PI3K)—*w;UAS-PI3K UAS-Aβ*/+*. Experimental genotypes were *w;elav-Gal4/UAS-Aβ** for Aβ-expressing flies, *w;elav-Gal4/UAS-PI3K UAS-Aβ** for flies co-expressing Aβ and high PI3K levels, and *w;elav-Gal4/UAS-PI3K* for flies with elevated PI3K. Each data point represents the average of 7–10 samples of the same genotype/age ±SEM. Logarithmic transformation of the data rendered a normal distribution, and thus was used for the ANOVA analysis, which showed a main effect of genotype ($F_{14,226} = 10.044$, $p < 0.001$) and age ($F_{1,226} = 4.156$, $p = 0.04$), but not of their interaction ($F_{14,226} = 1.370$, $p = 0.169$). Asterisks denote significant differences (** $p < 0.01$) with the other genotypes. Notice that overexpression of PI3K can rescue neurodegeneration induced by Aβ42, but not by Aβ42arc.

<https://doi.org/10.1371/journal.pone.0177541.g005>

Experiment Aβ40+PI3K: $\chi^2 = 14.95$, $p = 0.002$), which points to a possible neuroprotective effect of this peptide. In contrast, Aβ42 significantly reduced survival rate ($p < 0.001$ vs. all other genotypes)(Fig 6B), as has been previously shown [21–23,26,46]. Simultaneous expression of Aβ42 and PI3K reduced longevity even further ($p < 0.001$ vs. all other genotypes) (Fig 6B), indicating a synergistic deleterious effect between the two. In line with earlier studies [22,23,25,26,47], Aβ42arc showed the highest toxicity in this assay, which was not affected by the level of PI3K expression (Experiment Aβ42arc vs. Experiment Aβ42arc+PI3K $\chi^2 = 6.25$, $p = 0.1738$; $p < 0.001$ for both vs. all other genotypes)(Fig 6C). Thus, overexpression of PI3K

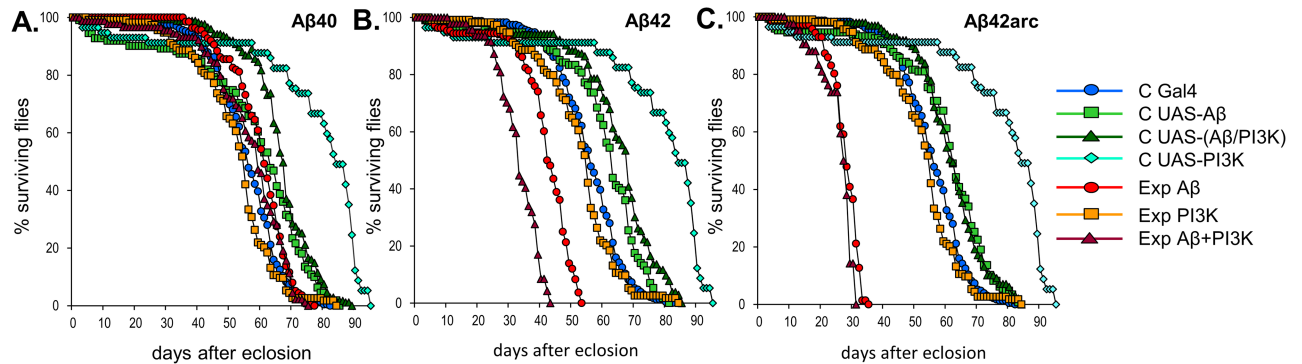


Fig 6. Effect of neuronal expression of three amyloid peptides, with or without overactivated PI3K signaling, on *Drosophila* life span. Life span was measured for males expressing A β 40 (A), A β 42 (B), or A β 42arc (C) with normal (Exp A β : genotype *w*; *D42-Gal4/UAS-A β **) or elevated levels of PI3K (Exp A β +PI3K: genotype *w*; *D42-Gal4/UAS-PI3K UAS-A β **), and in control males (C Gal4: *w*; *D42-Gal4/+*, C UAS-A β : *w*; *UAS-A β */+*, C UAS-PI3K: *w*; *UAS-PI3K/+*, C UAS-(A β /PI3K): *w*; *UAS-PI3K UAS-A β */+*) and PI3K-overexpressing males (Exp PI3K: *w*; *D42-Gal4/UAS-PI3K*). Differences in survival were analyzed using Kaplan-Meier survival plots and log-rank analysis (see Results for details). For each genotype, at least five experiments were performed with an average of 20 flies/experiment.

<https://doi.org/10.1371/journal.pone.0177541.g006>

does not seem to reduce A β toxicity in longevity assays. In summary, our data reveal that the implication of the PI3K pathway in the toxicity of A β differs for different A β species and in different contexts (synapse formation, cytotoxicity, and life span).

Discussion

Synapse dysfunction and loss are key to dementia in Alzheimer’s disease (AD). It is currently established that amyloid- β peptides are important contributors to these synaptic alterations, but the precise identity of the A β species involved is not well defined [10,49]. Likewise, it is unclear how aging, the most influential non-genetic risk factor in AD, influences A β synaptotoxicity. These are relevant questions to designing suitable therapeutic strategies. We postulated that the *Drosophila* adult glutamatergic neuromuscular junction (NMJ) would provide an ideal system in which to address these issues, because its stereotypic morphology would allow uncovering subtle albeit relevant changes. Moreover, our work has revealed a temporal biphasic process of synaptic remodeling at the adult NMJ. An early phase of net synapse addition takes place during the first two weeks of adult life, a critical time period in which several areas of the young fly brain have been shown to undergo experience-dependent structural plasticity [29,50,51]. Thenceforth, net synaptic elimination occurs, consistent with the onset of behavioural and synaptic senescence [31,32,50,52]. Thus, this model allows assessing A β influence on synaptic dynamics during synaptic maturation and aging. In this model we show that: (1) A β 40 seems to reduce the number of synaptic contacts by preventing synapse addition; (2) A β 42 synaptotoxicity gradually increases with age; and (3) A β 42arc produces net synaptic loss from early adulthood, but does not impede synapse addition. In summary, we demonstrate specific age-dependent synaptic effects for each A β peptide, and establish the fly adult NMJ as a suitable model to investigate the mechanisms underlying these peculiarities.

Early amyloid synaptotoxicity or a physiological role for A β ?

Studies in *Drosophila* had shown early memory defects induced by expression of both A β 40 and A β 42-derived peptides [19,20,22,23], but a structural and/or functional synaptic correlate had only been found for A β 42-derived peptides [19,20,25,26]. Here, we show for the first time that A β 40 reduces the number of synaptic contacts, and it seems to do so by preventing the

addition of new synapses that normally occurs in the adult NMJ. At young ages (3–15 days), A β 42 effect was remarkably similar to A β 40, which suggests that early in life, A β 42 may act similarly to A β 40 by opposing synapse addition. However, A β 42-expressing brains had the lowest amount of total peptide, which might explain these relatively mild early effects. In contrast, the mutant amyloid peptide A β 42arc elicited net synaptic loss also at young ages, yet it showed a pattern of age-dependent variation in synapse number similar to controls, indicating that it does not hinder synapse addition. These are significant qualitative differences that point to a physiological role for wild type amyloid species in the process of synaptic plasticity.

In general, exposure to A β is associated with weakening of synapses, which is consistent with a postulated A β function in promoting activity-dependent synaptic elimination during mammalian postnatal development [16]. Our data suggest that rather than eliciting synapse removal, A β 40, and possibly A β 42, prevents the formation and/or maturation of new synapses in *Drosophila*. Interestingly, early defects in ocular dominance plasticity in *APP^{swe}* transgenic mice, which generate elevated levels of wild type amyloid species, are associated with reduced strengthening and expansion of non-deprived eye cortical representations, while deprived eye weakening remains intact [53]. These data argue in favor of a similar effect for A β at synapses from juvenile mice and flies. In the *Drosophila* larval NMJ, the transition from immature to mature synapse involves changes in the relative contribution of specific glutamate receptors in postsynaptic receptor fields opposed to presynaptic active zones [54]. In mammals, synaptic elimination and maturation also involves changes in expression and trafficking of AMPA and NMDA glutamate receptors [55], a process that can be altered by A β [5,56–58]. The model described in this work represents an invaluable tool for genetically assessing the contribution of Glutamate receptors, and other molecules, in the amyloid-dependent alterations of synaptic refinement.

Although we cannot provide a mechanistic basis for the specific synaptotoxic activities of each A β species, the data on NMJs overexpressing PI3K suggest the direct implication of this pathway. First, despite its strong synaptogenic activity, PI3K over expression was not able to block A β -induced synaptic reduction. Second, western quantification showed that the activity of the pathway is reduced by A β expression, which is consistent with data from mammalian systems that suggest that amyloid peptides block Akt activation downstream of the PI3K enzyme [44,45], and increase GSK3 activity [43]. Moreover, the degree of PI3K pathway inhibition correlated with the extent of synaptic reduction, both being maximum for A β 42arc. Altogether, evidences point to a direct relationship between A β and the PI3K/Akt/GSK3 pathway as central to A β -induced synaptic dysfunction, but further studies would be necessary to unambiguously prove it. The importance of this matter is underscored by the relevance of GSK3 in AD, which has been used as a therapeutic target [42,43].

Aging and amyloid synaptotoxicity

The risk of AD increases with age, but the link between aging and A β toxicity is not fully understood. We have shown that after a stage of synaptic growth, synaptic elimination commences in the fly NMJ sometime between 15 and 20 days after eclosion. This age also represents a point of transition from growth to retraction for the abdominal longitudinal NMJ [27] and the mushroom bodies [30], and thus defines an age-dependent change in synaptic dynamics. Our data suggest that this age also delimits a change in the synaptic action of A β 42, which would oppose synapse addition in early adulthood, but cause synaptic removal in aged flies. In contrast, A β 42arc induces net synaptic loss at a similar rate at all ages tested, while A β 40 maintains an unvarying number of active sites at least until 30 days. These data suggest that the impact of age on A β synaptotoxicity differs for each amyloid species. Understanding the

mechanisms underlying age-dependent synaptic changes in wild type adult NMJs will be necessary for explaining the observed effects.

Several *in vitro* and *in vivo* studies have demonstrated different aggregation kinetics for the three A β species, which result in higher effective concentrations of specific aggregation forms with diverse toxic activities. Specifically, a recent *in vivo* study expressing tandem dimeric A β peptides in *Drosophila* has shown that the aggregation kinetics of A β 42 favors a relatively high population of toxic oligomeric species, while this population is undetectable for A β 40, which seems to more rapidly transit from monomeric to insoluble inert forms [59]. The E22G mutation in A β 42arc has been shown to accelerate both A β oligomerization and fibrillogenesis [60,61]. Thus, it is tempting to speculate that A β monomeric forms inhibit synapse addition, while oligomeric forms promote synapse removal. Assessing the synaptic effects of the various tandem dimeric A β peptides [59] on the *Drosophila* adult NMJ would provide invaluable data to test this hypothesis.

Amyloid-dependent synaptotoxicity, cytotoxicity, and life span shortening

Multiple studies in *Drosophila*, and in other models, suggest that the mechanisms underlying A β synaptotoxicity, cytotoxicity, and reduction of life span are different [19,22,23,46,47]. Even more, *in vivo* data demonstrate that manipulations that alter aggregation propensity can induce qualitative, rather than quantitative, shifts in the pathology induced [24]. Our data provide further support to this notion. First, we show that A β 40 disturbs synapses, but not cell survival or life span. Second, neurodegeneration levels were similar in 20 day-old flies expressing either A β 42 or A β 42arc, yet both genotypes displayed dramatically different life expectancy. Third, over expression of PI3K reduced early A β 42 cytotoxicity, measured by degree of neurodegeneration, but it enhanced the deleterious effects of this peptide on life span.

The differential effect of PI3K hyperactivation on A β -related phenotypic outcomes is intriguing. PI3K is an essential signaling pathway with multiple developmental and physiological functions; these include widespread functions such as regulation of cell proliferation and metabolism, or control of cellular remodeling and migration, but also cell-type specific roles such as synapse plasticity in neurons [62]. Moreover, different levels of pathway activation seems to trigger distinct responses [63,64]. In view of this complexity, we can only speculate on how PI3K alters A β -induced phenotypes. Our data show that PI3K overexpression had no influence on A β 42arc-related phenotypes, a finding that might well be explained by the significant reduction in the activity of the PI3K pathway displayed by A β 42arc-expressing flies. In contrast, the observed reduced neurodegeneration in flies co-expressing A β 42 and PI3K could reflect residual hyper-activation of the pro-survival PI3K pathway, as suggested by western quantification. This hypothesis is consistent with studies in mice which suggest that low levels of Akt activity are sufficient to support neuronal survival responses [64]. However, PI3K overexpression had a negative effect on life span in flies expressing A β 42. Lifespan is an extremely complex trait which may be particularly sensitive to unbalanced conditions, and age-dependent accumulation of toxic amyloid aggregates might further disturb PI3K and related signaling networks, advancing deterioration. These data underscore the complexity of A β toxicity and the necessity to test it at different levels when assessing the consequences of therapeutic approaches.

In summary, using an *in vivo* model we demonstrate that (1) different amyloid species disturb synapses by differentially influencing synapse addition or synapse elimination, (2) age-dependent changes in their synaptotoxicity are species-specific, and (3) the toxic actions of each A β peptide differ in different contexts. Furthermore, our work demonstrates the value of

the *Drosophila* adult NMJ as an ideal *in vivo* model for understanding specific effects of amyloid peptides on synaptic plasticity.

Acknowledgments

We thank DC. Crowther, the Developmental Studies Hybridoma Bank, and the Bloomington Stock Center for antibodies and fly lines, A.B. Fernández, M. Ruiz, and J. Benito for reagents, and A. Ferrús and A. Acebes for comments on the manuscript.

Author Contributions

Conceptualization: IC LT.

Formal analysis: BLA IM LT ET.

Funding acquisition: IC LT.

Investigation: BLA LT.

Project administration: LT.

Software: IM.

Supervision: LT.

Visualization: BLA ET LT.

Writing – original draft: BLA ET LT.

Writing – review & editing: LT.

References

1. Selkoe DJ. Alzheimer's disease is a synaptic failure. *Science*. 2002; 298(5594):789–91. <https://doi.org/10.1126/science.1074069> PMID: 12399581
2. Shankar GM, Li S, Mehta TH, Garcia-Munoz A, Shepardson NE, Smith I, et al. Amyloid-beta protein dimers isolated directly from Alzheimer's brains impair synaptic plasticity and memory. *Nat Med*. 2008; 14(8):837–42. <https://doi.org/10.1038/nm1782> PMID: 18568035
3. Walsh DM, Klyubin I, Fadeeva JV, Cullen WK, Anwyl R, Wolfe MS, et al. Naturally secreted oligomers of amyloid beta protein potently inhibit hippocampal long-term potentiation in vivo. *Nature*. 2002; 416(6880):535–9. <https://doi.org/10.1038/416535a> PMID: 11932745
4. Lacor PN, Buniel MC, Furlow PW, Clemente AS, Velasco PT, Wood M, et al. Abeta oligomer-induced aberrations in synapse composition, shape, and density provide a molecular basis for loss of connectivity in Alzheimer's disease. *J Neurosci Off J Soc Neurosci*. 2007; 27(4):796–807.
5. Shankar GM, Bloodgood BL, Townsend M, Walsh DM, Selkoe DJ, Sabatini BL. Natural oligomers of the Alzheimer amyloid-beta protein induce reversible synapse loss by modulating an NMDA-type glutamate receptor-dependent signaling pathway. *J Neurosci Off J Soc Neurosci*. 2007; 27(11):2866–75.
6. Lesné S, Koh MT, Kotilinek L, Kaye R, Glabe CG, Yang A, et al. A specific amyloid-beta protein assembly in the brain impairs memory. *Nature*. 2006; 440(7082):352–7. <https://doi.org/10.1038/nature04533> PMID: 16541076
7. McDonald MP, Dahl EE, Overmier JB, Mantyh P, Cleary J. Effects of an exogenous beta-amyloid peptide on retention for spatial learning. *Behav Neural Biol*. 1994; 62(1):60–7. PMID: 7945146
8. Ma T, Klann E. Amyloid β : linking synaptic plasticity failure to memory disruption in Alzheimer's disease. *J Neurochem*. 2012; 120:140–8. <https://doi.org/10.1111/j.1471-4159.2011.07506.x> PMID: 22122128
9. Wilcox K, Lacor P, Pitt J, Klein W. A β Oligomer-Induced Synapse Degeneration in Alzheimer's Disease. *Cell Mol Neurobiol*. 2011; 31(6):939–48. <https://doi.org/10.1007/s10571-011-9691-4> PMID: 21538118
10. Benilova I, Karran E, De Strooper B. The toxic A β oligomer and Alzheimer's disease: an emperor in need of clothes. *Nat Neurosci*. 2012; 15(3):349–57. <https://doi.org/10.1038/nn.3028> PMID: 22286176

11. Kamenetz F, Tomita T, Hsieh H, Seabrook G, Borchelt D, Iwatsubo T, et al. APP processing and synaptic function. *Neuron*. 2003; 37(6):925–37. PMID: [12670422](https://pubmed.ncbi.nlm.nih.gov/12670422/)
12. Garcia-Osta A, Alberini CM. Amyloid beta mediates memory formation. *Learn Mem*. 2009; 16(4): 267–72. <https://doi.org/10.1101/lm.1310209> PMID: [19318468](https://pubmed.ncbi.nlm.nih.gov/19318468/)
13. Abramov E, Dolev I, Fogel H, Ciccotosto GD, Ruff E, Slutsky I. Amyloid- β as a positive endogenous regulator of release probability at hippocampal synapses. *Nat Neurosci*. 2009; 12(12):1567–76. <https://doi.org/10.1038/nn.2433> PMID: [19935655](https://pubmed.ncbi.nlm.nih.gov/19935655/)
14. Puzzo D, Privitera L, Leznik E, Fa M, Staniszewski A, Palmeri A, et al. Picomolar Amyloid- β Positively Modulates Synaptic Plasticity and Memory in Hippocampus. *J Neurosci*. 2008; 28(53):14537–45. <https://doi.org/10.1523/JNEUROSCI.2692-08.2008> PMID: [19118188](https://pubmed.ncbi.nlm.nih.gov/19118188/)
15. Puzzo D, Privitera L, Fa' M, Staniszewski A, Hashimoto G, Aziz F, et al. Endogenous amyloid- β is necessary for hippocampal synaptic plasticity and memory. *Ann Neurol*. 2011; 69(5):819–30. <https://doi.org/10.1002/ana.22313> PMID: [21472769](https://pubmed.ncbi.nlm.nih.gov/21472769/)
16. Wasling P, Daborg J, Riebe I, Andersson M, Portelius E, Blennow K, et al. Synaptic Retrogenesis and Amyloid- β in Alzheimer's Disease. *J Alzheimers Dis*. 1 2009; 16(1):1–14. <https://doi.org/10.3233/JAD-2009-0918> PMID: [19158416](https://pubmed.ncbi.nlm.nih.gov/19158416/)
17. Iijima-Ando K, Iijima K. Transgenic *Drosophila* models of Alzheimer's disease and tauopathies. *Brain Struct Funct*. 2010; 214(2–3):245–62. <https://doi.org/10.1007/s00429-009-0234-4> PMID: [19967412](https://pubmed.ncbi.nlm.nih.gov/19967412/)
18. Moloney A, Sattelle DB, Lomas DA, Crowther DC. Alzheimer's disease: insights from *Drosophila melanogaster* models. *Trends Biochem Sci*. 2010; 35(4):228–35. <https://doi.org/10.1016/j.tibs.2009.11.004> PMID: [20036556](https://pubmed.ncbi.nlm.nih.gov/20036556/)
19. Chiang H-C, Wang L, Xie Z, Yau A, Zhong Y. PI3 kinase signaling is involved in A β -induced memory loss in *Drosophila*. *Proc Natl Acad Sci*. 2010; 107(15):7060–5. <https://doi.org/10.1073/pnas.0909314107> PMID: [20351282](https://pubmed.ncbi.nlm.nih.gov/20351282/)
20. Fang L, Duan J, Ran D, Fan Z, Yan Y, Huang N, et al. Amyloid- β depresses excitatory cholinergic synaptic transmission in *Drosophila*. *Neurosci Bull*. 2012; 28(5):585–94. <https://doi.org/10.1007/s12264-012-1267-x> PMID: [23054636](https://pubmed.ncbi.nlm.nih.gov/23054636/)
21. Crowther DC, Kinghorn KJ, Miranda E, Page R, Curry JA, Duthie FAI, et al. Intraneuronal A β , non-amyloid aggregates and neurodegeneration in a *Drosophila* model of Alzheimer's disease. *Neuroscience*. 2005; 132(1):123–35. <https://doi.org/10.1016/j.neuroscience.2004.12.025> PMID: [15780472](https://pubmed.ncbi.nlm.nih.gov/15780472/)
22. Iijima K, Liu H-P, Chiang A-S, Hearn SA, Konsolaki M, Zhong Y. Dissecting the pathological effects of human A β 40 and A β 42 in *Drosophila*: A potential model for Alzheimer's disease. *Proc Natl Acad Sci U S A*. 2 2004; 101(17):6623–8. <https://doi.org/10.1073/pnas.0400895101> PMID: [15069204](https://pubmed.ncbi.nlm.nih.gov/15069204/)
23. Iijima K, Chiang H-C, Hearn SA, Hakker I, Gatt A, Shenton C, et al. A β 42 Mutants with Different Aggregation Profiles Induce Distinct Pathologies in *Drosophila*. *PLoS ONE*. 2008; 3(2):e1703. <https://doi.org/10.1371/journal.pone.0001703> PMID: [18301778](https://pubmed.ncbi.nlm.nih.gov/18301778/)
24. Luheshi LM, Tartaglia GG, Brorsson A-C, Pawar AP, Watson IE, Chiti F, et al. Systematic In Vivo Analysis of the Intrinsic Determinants of Amyloid β Pathogenicity. *PLoS Biol*. 3 2007; 5(11):e290. <https://doi.org/10.1371/journal.pbio.0050290> PMID: [17973577](https://pubmed.ncbi.nlm.nih.gov/17973577/)
25. Sofola O, Kerr F, Rogers I, Killick R, Augustin H, Gandy C, et al. Inhibition of GSK-3 Ameliorates A β Pathology in an Adult-Onset *Drosophila* Model of Alzheimer's Disease. *PLoS Genet*. 2010; 6(9): e1001087. <https://doi.org/10.1371/journal.pgen.1001087> PMID: [20824130](https://pubmed.ncbi.nlm.nih.gov/20824130/)
26. Zhao X-L, Wang W-A, Tan J-X, Huang J-K, Zhang X, Zhang B-Z, et al. Expression of β -Amyloid Induced Age-Dependent Presynaptic and Axonal Changes in *Drosophila*. *J Neurosci*. 2010; 30(4):1512–22. <https://doi.org/10.1523/JNEUROSCI.3699-09.2010> PMID: [20107079](https://pubmed.ncbi.nlm.nih.gov/20107079/)
27. Beramendi A, Peron S, Casanova G, Reggiani C, Cantera R. Neuromuscular junction in abdominal muscles of *Drosophila melanogaster* during adulthood and aging. *J Comp Neurol*. 2007; 501(4): 498–508. <https://doi.org/10.1002/cne.21253> PMID: [17278125](https://pubmed.ncbi.nlm.nih.gov/17278125/)
28. Rivlin PK, Clair RMS, Vilinsky I, Deitcher DL. Morphology and molecular organization of the adult neuromuscular junction of *Drosophila*. *J Comp Neurol*. 2004; 468(4):596–613. <https://doi.org/10.1002/cne.10977> PMID: [14689489](https://pubmed.ncbi.nlm.nih.gov/14689489/)
29. Devaud J-M, Acebes A, Ramaswami M, Ferrús A. Structural and functional changes in the olfactory pathway of adult *Drosophila* take place at a critical age. *J Neurobiol*. 2003; 56(1):13–23. <https://doi.org/10.1002/neu.10215> PMID: [12767029](https://pubmed.ncbi.nlm.nih.gov/12767029/)
30. Technau GM. Fiber number in the mushroom bodies of adult *Drosophila melanogaster* depends on age, sex and experience. *J Neurogenet*. 1984; 1(2):113–26. PMID: [6085635](https://pubmed.ncbi.nlm.nih.gov/6085635/)
31. Grotewiel MS, Martin I, Bhandari P, Cook-Wiens E. Functional senescence in *Drosophila melanogaster*. *Ageing Res Rev*. 2005; 4(3):372–97. <https://doi.org/10.1016/j.arr.2005.04.001> PMID: [16024299](https://pubmed.ncbi.nlm.nih.gov/16024299/)

32. Iliadi KG, Boulianne GL. Age-related behavioral changes in *Drosophila*. *Ann N Y Acad Sci*. 2010; 1197(1):9–18.
33. Nilsberth C, Westlind-Danielsson A, Eckman CB, Condron MM, Axelman K, Forsell C, et al. The «Arctic» APP mutation (E693G) causes Alzheimer's disease by enhanced A β protofibril formation. *Nat Neurosci*. 2001; 4(9):887–93. <https://doi.org/10.1038/nn0901-887> PMID: 11528419
34. Martín-Peña A, Acebes A, Rodríguez J-R, Sorribes A, de Polavieja GG, Fernández-Fúnez P, et al. Age-Independent Synaptogenesis by Phosphoinositide 3 Kinase. *J Neurosci*. 2006; 26(40):10199–208. <https://doi.org/10.1523/JNEUROSCI.1223-06.2006> PMID: 17021175
35. Legan SK, Rebrin I, Mockett RJ, Radyuk SN, Klichko VI, Sohal RS, et al. Overexpression of Glucose-6-phosphate Dehydrogenase Extends the Life Span of *Drosophila melanogaster*. *J Biol Chem*. 2008; 283(47):32492–9. <https://doi.org/10.1074/jbc.M805832200> PMID: 18809674
36. Leever SJ, Weinkove D, MacDougall LK, Hafen E, Waterfield MD. The *Drosophila* phosphoinositide 3-kinase Dp110 promotes cell growth. *EMBO J*. 1996; 15(23):6584–94. PMID: 8978685
37. Hebbar S, Hall RE, Demski SA, Subramanian A, Fernandes JJ. The adult abdominal neuromuscular junction of *Drosophila*: A model for synaptic plasticity. *J Neurobiol*. 2006; 66(10):1140–55. <https://doi.org/10.1002/neu.20279> PMID: 16838368
38. Wagh DA, Rasse TM, Asan E, Hofbauer A, Schwenkert I, Dürrbeck H, et al. Bruchpilot, a protein with homology to ELKS/CAST, is required for structural integrity and function of synaptic active zones in *Drosophila*. *Neuron*. 2006; 49(6):833–44. <https://doi.org/10.1016/j.neuron.2006.02.008> PMID: 16543132
39. McGurk L, Morrison H, Keegan LP, Sharpe J, O'Connell MA. Three-dimensional imaging of *Drosophila melanogaster*. *PLoS One*. 2007; 2(9):e834. <https://doi.org/10.1371/journal.pone.0000834> PMID: 17786206
40. Yang J-S, Nam H-J, Seo M, Han SK, Choi Y, Nam HG, et al. OASIS: Online Application for the Survival Analysis of Lifespan Assays Performed in Aging Research. *PLoS ONE*. 2011; 6(8):e23525. <https://doi.org/10.1371/journal.pone.0023525> PMID: 21858155
41. Cuesto G, Enriquez-Barreto L, Caramés C, Cantarero M, Gasull X, Sandi C, et al. Phosphoinositide-3-Kinase Activation Controls Synaptogenesis and Spinogenesis in Hippocampal Neurons. *J Neurosci*. 2011; 31(8):2721–33. <https://doi.org/10.1523/JNEUROSCI.4477-10.2011> PMID: 21414895
42. Kremer A, Louis JV, Jaworski T, Van Leuven F. GSK3 and Alzheimer's Disease: Facts and Fiction. ... *Front Mol Neurosci*. 2011; 4:17. <https://doi.org/10.3389/fnmol.2011.00017> PMID: 21904524
43. Llorens-Martín M, Jurado J, Hernández F, Avila J. GSK-3 β , a pivotal kinase in Alzheimer disease. *Front Mol Neurosci*. 2014; 7:46. <https://doi.org/10.3389/fnmol.2014.00046> PMID: 24904272
44. Lee H-K, Kumar P, Fu Q, Rosen KM, Querfurth HW. The insulin/Akt signaling pathway is targeted by intracellular beta-amyloid. *Mol Biol Cell*. 2009; 20(5):1533–44. <https://doi.org/10.1091/mbc.E08-07-0777> PMID: 19144826
45. Jimenez S, Torres M, Vizuete M, Sanchez-Varo R, Sanchez-Mejias E, Trujillo-Estrada L, et al. Age-dependent accumulation of soluble amyloid beta (A β) oligomers reverses the neuroprotective effect of soluble amyloid precursor protein-alpha (sAPP(alpha)) by modulating phosphatidylinositol 3-kinase (PI3K)/Akt-GSK-3beta pathway in Alzheimer mouse model. *J Biol Chem*. 2011; 286(21):18414–25. <https://doi.org/10.1074/jbc.M110.209718> PMID: 21460223
46. Costa R, Speretta E, Crowther DC, Cardoso I. Testing the therapeutic potential of doxycycline in a *Drosophila melanogaster* model of Alzheimer's disease. *J Biol Chem* 2011; 286(48): 41647–55. <https://doi.org/10.1074/jbc.M111.274548> PMID: 21998304
47. Kerr F, Augustin H, Piper MDW, Gandy C, Allen MJ, Lovestone S, et al. Dietary restriction delays aging, but not neuronal dysfunction, in *Drosophila* models of Alzheimer's disease. *Neurobiol Aging*. 2011; 32(11):1977–89. <https://doi.org/10.1016/j.neurobiolaging.2009.10.015> PMID: 19969390
48. Brunet A, Datta SR, Greenberg ME. Transcription-dependent and -independent control of neuronal survival by the PI3K-Akt signaling pathway. *Curr Opin Neurobiol*. junio de 2001; 11(3):297–305.
49. Shankar GM, Walsh DM. Alzheimer's disease: synaptic dysfunction and A β . *Mol Neurodegener*. 2009; 4:48. <https://doi.org/10.1186/1750-1326-4-48> PMID: 19930651
50. Donlea JM, Ramanan N, Silverman N, Shaw PJ. Genetic Rescue of Functional Senescence in Synaptic and Behavioral Plasticity. *Sleep*. 2014; 37(9):1427–37. <https://doi.org/10.5665/sleep.3988> PMID: 25142573
51. Heisenberg M, Heusipp M, Wanke C. Structural plasticity in the *Drosophila* brain. *J Neurosci Off J Soc Neurosci*. 1995; 15(3 Pt 1):1951–60.
52. Haddadi M, Jahromi SR, Sagar BKC, Patil RK, Shivanandappa T, Ramesh SR. Brain aging, memory impairment and oxidative stress: a study in *Drosophila melanogaster*. *Behav Brain Res*. 2014; 259: 60–9. <https://doi.org/10.1016/j.bbr.2013.10.036> PMID: 24183945

53. William CM, Andermann ML, Goldey GJ, Roumis DK, Reid RC, Shatz CJ, et al. Synaptic Plasticity Defect Following Visual Deprivation in Alzheimer's Disease Model Transgenic Mice. *J Neurosci*. 2012; 32(23):8004–11. <https://doi.org/10.1523/JNEUROSCI.5369-11.2012> PMID: 22674275
54. Thomas U, Sigrist SJ. Glutamate receptors in synaptic assembly and plasticity: case studies on fly NMJs. *Adv Exp Med Biol*. 2012; 970:3–28. https://doi.org/10.1007/978-3-7091-0932-8_1 PMID: 22351049
55. McKinney RA. Excitatory amino acid involvement in dendritic spine formation, maintenance and remodeling. *J Physiol*. 2010; 588(Pt 1):107–16. <https://doi.org/10.1113/jphysiol.2009.178905> PMID: 19933758
56. Almeida CG, Tampellini D, Takahashi RH, Greengard P, Lin MT, Snyder EM, et al. Beta-amyloid accumulation in APP mutant neurons reduces PSD-95 and GluR1 in synapses. *Neurobiol Dis*. 2005; 20(2): 187–98. <https://doi.org/10.1016/j.nbd.2005.02.008> PMID: 16242627
57. Hsieh H, Boehm J, Sato C, Iwatsubo T, Tomita T, Sisodia S, et al. AMPAR removal underlies Abeta-induced synaptic depression and dendritic spine loss. *Neuron*. 2006; 52(5):831–43. <https://doi.org/10.1016/j.neuron.2006.10.035> PMID: 17145504
58. Snyder EM, Nong Y, Almeida CG, Paul S, Moran T, Choi EY, et al. Regulation of NMDA receptor trafficking by amyloid-beta. *Nat Neurosci*. 2005; 8(8):1051–8. <https://doi.org/10.1038/nn1503> PMID: 16025111
59. Speretta E, Jahn TR, Tartaglia GG, Favrin G, Barros TP, Imarisio S, et al. Expression in *Drosophila* of Tandem A β Peptides Provides Insights Into the Link Between Aggregation and Neurotoxicity. *J Biol Chem* 2012; 287(24):20748–54. <https://doi.org/10.1074/jbc.M112.350124> PMID: 22461632
60. Brorsson A-C, Bolognesi B, Tartaglia GG, Shammass SL, Favrin G, Watson I, et al. Intrinsic Determinants of Neurotoxic Aggregate Formation by the Amyloid β Peptide. *Biophys J*. 2010; 98(8):1677–84. <https://doi.org/10.1016/j.bpj.2009.12.4320> PMID: 20409489
61. Norlin N, Hellberg M, Filippov A, Sousa AA, Gröbner G, Leapman RD, et al. Aggregation and fibril morphology of the Arctic mutation of Alzheimer's A β peptide by CD, TEM, STEM and in situ AFM. *J Struct Biol*. 2012; 180(1):174–89. <https://doi.org/10.1016/j.jsb.2012.06.010> PMID: 22750418
62. Knafo S, Esteban JA. Common pathways for growth and for plasticity. *Curr Opin Neurobiol*. 2012; 22(3):405–11. <https://doi.org/10.1016/j.conb.2012.02.008> PMID: 22398399
63. Iwanami A, Cloughesy TF, Mischel PS. Striking the balance between PTEN and PDK1: it all depends on the cell context. *Genes Dev* 2009; 23:1699–704 <https://doi.org/10.1101/gad.1832909> PMID: 19651981
64. Zhou X, Cordon-Barris L, Zurashvili T, Bayascas JR. Fine-tuning the intensity of the PKB/Akt signal enables diverse physiological responses. *Cell Cycle*. 2014; 13(20):3164–8. <https://doi.org/10.4161/15384101.2014.962954> PMID: 25485494